OPTIMIZATION DESIGN OF AN AIR-PRESSURE SUBSOILER TYPE
/
气吹式深松铲优化与设计

Hongjie Su, Hongmei Cui*, Feiyu Li, Teng Fan
College of Mechanical and Electrical Engineering, Inner Mongolia Agricultural University, Hohhot, China
Tel：+86 18686001276；E-mail: chm123m@126.com
DOI: https://doi.org/10.35633/inmateh-63-15

Keywords: *subsoiler, soil bulk density, air-pressure subsoiler, specific draft force*

ABSTRACT
Through the mechanical analysis of air-pressure subsoiler, it is found that the main factors affecting its tractive resistance are the air pressure injected into the soil, the soil cohesion, the length and width of the shovel surface, the soil disturbance coefficient, and moving speed of the subsoiler. The traditional air-pressure subsoiler was redesigned to solve the problem of large tractive resistance. In the soil trench experiment, the subsoiling shovel's shape, the air pressure, and the position of air hole were used as test factors, and the ratio of the traction resistance of the shovel to the soil disturbance, namely SDF (Specific Draft Force), was used as the evaluation index. By the response surface test method and analysing the soil disturbance and the tractive resistance, it is determined that rectangular subsoiling shovel with the air hole in the upper part of the shovel is the optimal under the pressure of 1.2 MPa.

摘要
针对气吹式深松铲阻力大的问题，通过对气压式深松铲力学分析，确定影响牵引阻力的因素主要有，注入土壤内部的气压大小、土壤的内聚力、铲面的长度与宽度、土壤扰动系数以及深松铲行进速度。重新设计气压式深松铲，在土槽实验室中以深松铲铲形，气压大小，与气孔位置为试验因素，以深松铲牵引阻力与深松土壤扰动量的比值即比阻 SDF 为评价指标，使用响应面试验方法，综合深松土壤的扰动量与深松铲的牵引阻力进行优化分析，最终确定凿式深松铲加压 1.2Mpa 气孔位置在上部时为相对最优的深松铲。

INTRODUCTION

Since the soil plough pan and soil compaction are becoming increasingly serious (*An Jing, 2016*), it is urgent to improve soil compaction and break the plough pan. Air-Pressure subsoilers (*Zuo Shengjia et al., 2017*) can not only break the plough pan, but also reduce the soil bulk density, improve soil compaction, and provide suitable conditions for crop growth.

European countries adopted subsoil technology early (*Zhang Si, 2018*). In the 1930s, vibrating subsoilers, combined working machines and other agricultural machinery and tools were widely applied in most European countries. A large number of studies have shown (*Bandalan E.P. et al., 1999; Niyamapa T. et al., 2000; Wang Y.X. et al., 2019*) that the vibrating subsoiler can reduce the resistance of the subsoiler, and the forced vibrating subsoiler can reduce the tractive resistance. The self-excited vibrating subsoiler, despite being capable of reducing the tractive resistance, is subject to unstable tillage depth and easy deviation of the frame, so its structural reliability needs to be improved.

Since the 1960s, some scholars and institutions in China have begun to study the structure and mechanism of subsoilers. Based on domestic and foreign subsoiling technology research, China has developed a new type of subsoiling machine—Air-Pressure subsoiler. This subsoiler solves the problems of large subsoil resistance, high energy consumption, unstable subsoil depth and poor structural reliability of traditional subsoilers. The first application of high-pressure gas permeation was by the HSMRC team of NJIT in the United States. They injected high-pressure gas into the rock and soil to remove pollutants. Sehuring's experimental research on injecting high-pressure gas into the soil showed that the air flow rate and the pollutant penetration rate in the soil were increased by 6 times after the high-pressure gas was injected into the soil (*Zuo Shengjia et al., 2017; He Jin, 2005; Gao Xiaodong et al., 2015; Schuring J.R. et al., 1991*).

*Hongjie Su, MS.Stud. Eng.; Hongmei Cui *, Associate Prof, Ph.D. Eng.; Feiyu Li, MS.Stud.Eng；Teng Fan，MS.Stud.Eng.*

In 2016, Zuo developed a new type of air-pressure subsoiling machine. Air-Pressure subsoiling means to create cracks in the soil with high pressure gas during subsoiling so as to improve the porosity of the soil, thereby better crushing the soil. Studies have shown that subsoiling can not only break the plough pan, but also reduce the soil bulk density (*Zuo Shengjia et al., 2017*). In 2018, Liu et al. (*Liu Mingcai, 2018*) designed an air-pressure subsoiler suitable for clay in southern China.

At present, the studies on subsoilers mostly focus on vibrating subsoilers (*Hilal Y.Y et al., 2021; Wang Y. et al., 2019*), few of them being on air-pressure subsoilers. Air-Pressure subsoiling technique is in its infancy, and air-pressure subsoiler also has the problem of large subsoil resistance. To address this problem, it is urgent to optimize the original air-pressure subsoiler.

MATERIALS AND METHODS

Stress analysis of air-pressure subsoiler

It can be seen from Figure 1 that when the subsoiling shovel moves towards the left at a constant speed of v, the soil is pushed forward by it, which produces a shearing force that acts on the soil. And this shearing force will result in an instantaneous cohesion force CS and a friction force $\mu' N$ generated by the movement between the soil, as well as a friction force μN_2 between the soil and the shovel surface generated by the movement of the soil along the shovel surface. Different from traditional subsoiler, the proposed Air-Pressure subsoiler generates air pressure P that acts on the soil, and at the same time produces a reaction force of the same magnitude on the shovel surface.

When the Air-Pressure subsoiler moves forward, the force balance equation can be expressed as:

$$F = N_2 \cdot \sin\alpha + \mu N_2 \cdot \cos\alpha + R \cdot L + P \cdot L \cdot A \cdot \sin\alpha \quad (1)$$

where:

F is the tractive resistance, (N);

N_2 is the normal force on the shovel surface, (N);

μ is the friction coefficient between soil movement and the shovel surface;

R is the cutting force generated by the shovel surface moving forward on the soil, (N);

L is the width of the shovel surface, (m);

α is the angle between the shovel surface and the soil surface, (°);

A is the length of the air pressure distribution on the shovel surface when the air-pressure subsoiler is working, (m).

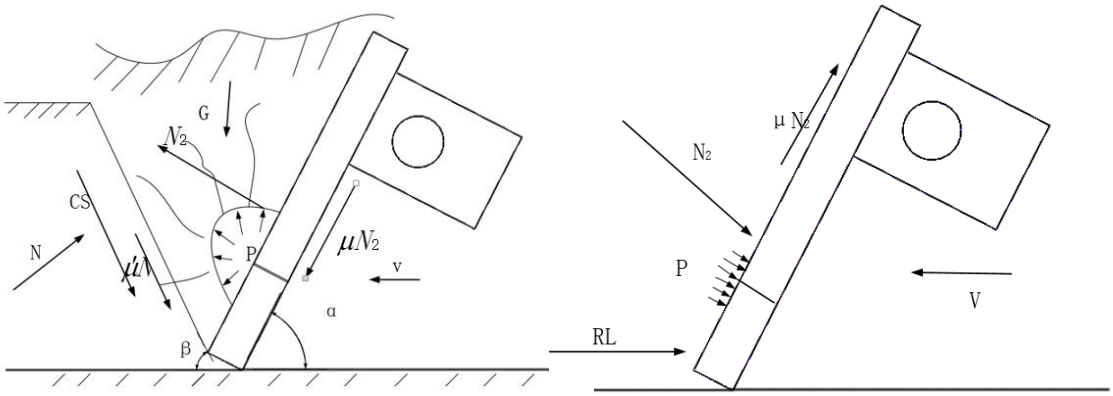

Fig. 1 - The force model of the shovel surface and the soil during the movement of the air-pressure subsoiler

If the soil block on the shovel surface during the movement of the Air-Pressure subsoiler is taken as the research object, the horizontal balance equation of the soil block at this time can be expressed as:

$$N_2(\sin\alpha + \mu'\cos\alpha) - N(\sin\beta + \mu L\cos\beta) - (CS + B - PS_1)\cos\beta = 0 \quad (2)$$

The vertical balance equation of the soil block can be written as:

$$G - N_2(\cos\alpha - \mu\sin\alpha) - N(\cos\beta - \mu'\sin\beta) + (CS + B - PS_1)\sin\beta = 0 \quad (3)$$

where: G is the gravity of the soil block on the shovel surface, (N);

N is the normal load acting on the front failure surface, (N);

B is the acceleration force generated by the movement of the soil block, (N);

β is the inclination of the front failure surface of the soil, (°);

μ' is the soil' internal friction coefficient;

CS is the cohesive force generated when the soil fails (N);

P is the air pressure of the air tube (Pa);

S_1 is the effective soil area raised by the air pressure (m²).

By establishing the simultaneous equations of the above formulas, N_0 and N_1 can be eliminated. Then we get:

$$M_2 = \frac{\cos\alpha - \mu\sin\alpha}{\sin\alpha + \mu\cos\alpha} + \frac{\cos\beta - \mu\sin\beta}{\sin\beta + \mu\cos\beta} \tag{4}$$

The tractive resistance of the subsoiler is finally obtained as:

$$F = \frac{G}{M_2} + \frac{CS + B - PS_1}{M_2(\sin\beta + \cos\beta)} + PLA\sin\alpha \tag{5}$$

According to the experimental study of soil pressure characteristics conducted by Zuo (*Zuo Shengjia et al., 2019*), the effective area of soil lifted by the shovel surface can be expressed as:

$$S_1 = \pi R^2 \tag{6}$$

where: R is a radius.

Based on the above formula and Guo's (*Guo Jinlong, 2016)* research on the relationship between soil velocity and geometry, the expression of the soil block's acceleration and that of the failure area of the soil block's front section can be derived:

$$G = f \cdot L \cdot d\frac{\sin(\alpha+\beta)}{\beta}\left[L1 + \frac{1}{2}\left(\frac{d\cdot\cos(\alpha+\beta)}{\beta} + L1\right)\right] \tag{7}$$

$$A = \frac{f}{g} L \cdot d \cdot t \cdot v^2 \frac{\sin\alpha}{\sin(\alpha+\beta)} \tag{8}$$

$$S = \frac{L\cdot d}{\sin\beta} \tag{9}$$

where: g is the acceleration of gravity (m/s²),

t is the time (s),

v is the speed of subsoiler (m/s),

f is the soil bulk density (kg/m³),

$L1$ is the length of shovel surface (m);

d is the soil disturbance coefficient (m).

The above formula is reorganized and brought into the formula of tractive resistance to get:

$$F = \frac{fLd\frac{\sin(\alpha+\beta)}{\beta}\left[L1 + \frac{1}{2}\left(\frac{d\cos(\alpha+\beta)}{\beta} + L1\right)\right]}{M_2} + \frac{\frac{CL\mathrm{d}}{\sin\beta} + \frac{f}{g}Ld\cdot tv^2\frac{\sin\alpha}{\sin(\alpha+\beta)} + P\pi R^2}{M_2(\sin\beta + \mu\cos\beta)} + PL\sin\alpha\frac{f}{g}Ldtv^2\frac{\sin\alpha}{\sin(\alpha+\beta)} \tag{10}$$

When the high-pressure gas enters the soil through the air tube of the Air-Pressure subsoiler, the air pressure acting on the soil partly counteracts the soil's cohesive force and the acceleration force on the shovel surface. It can be known from formula (10) that the main influencing factors of tractive resistance are: the air pressure injected into the soil, the cohesion of the soil, the length and width of the shovel surface, the soil disturbance coefficient, and the speed of the subsoiler.

Aiming at the problem of the large tractive resistance of the Air-Pressure subsoiler, a new type of air-pressure subsoiler is designed.

According to the above-mentioned mechanical analysis, the shape of the shovel, the magnitude of the air pressure, and the position of the air hole are the design factors, as shown in Figure 2. Three types of subsoiling shovel (rectangular, triangular, and rhombic) are designed. The magnitude of the Air-Pressure subsoiler's air pressure, the shape of the shovel, and the position of air hole on the shovel were used as test factors.

The soil trench test was conducted in the laboratory of Inner Mongolia Agricultural University. The disturbance of the soil after the soil was subsoiled by the air-pressure subsoiler was recorded. In the meantime, the tractive resistance of each group of subsoiling shovels was recorded through the force sensor installed on the six force suspension on the trolley.

The specific draft force (SDF) was calculated by Formula (11) which can be found on the next page.

Test Scheme

According to the above analysis, the shape of subsoiling shovel *A,* the magnitude of air pressure B (MPa), and the position of air hole C were chosen as the three test factors/levels.

The specific factors/levels in the test are shown in the table below.

Table 1

Levels of test factors

Level/factor	Shape of shovel	Air pressure (MPa)	Position of ventilation hole
1	Rectangular	0	upper
2	Triangular	0.6	middle
3	Rhombic	1.2	lower

A total of three shovel shapes were designed for the new Air-Pressure subsoiler, as shown in Figure 2.

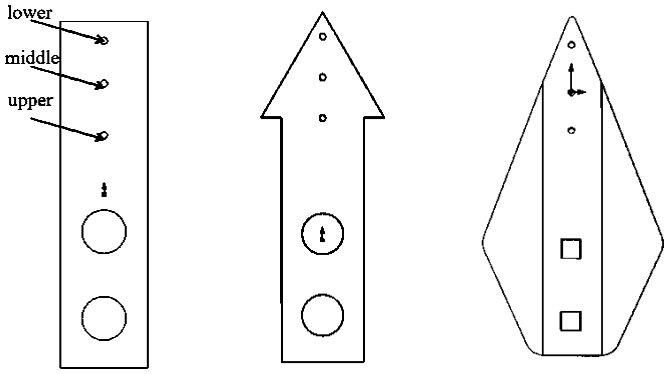

(a) Rectangular *(b) Triangular shovel* *(c) Rhombic shovel*

Fig. 2 - Shapes of shovel

From the *Agricultural Machinery Design Manual (Mechanical Research Institute of the First Ministry of Machinery*), it can be known that the subsoiling shovel's entry angle ranges from 18° to 24°. The research of Liu et al. (*Liu Jun 'an et al., 2018*) showed that when the shovel's entry angle is 21°, the subsoiling effect is the best and the tractive resistance is the smallest. Therefore, the shovel tip is fixed on the shovel shaft, so that the entry angle into the soil is 21°. The specific parameters are shown in Figure 3.

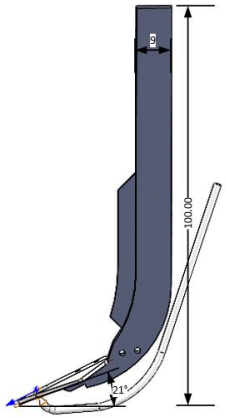

Fig. 3 - Structure of the Air-Pressure subsoiler

The 3D modelling software SolidWorks is applied to model the subsoiling shovel. It can be seen from Figure 3 that the rear of the shovel is connected to the air tube. The length is 100 cm, and the shovel handle is 9 cm in width.

SDF was selected as the evaluation index to evaluate the subsoiling effect of the shovel. With reference to the established groove area, the SDF was calculated by the formula of SDF.

$$SDF = F / A \tag{11}$$

where: SDF is the specific draft force to be calculated, (N/cm^2);

F is the tractive resistance, (N);

A is the soil disturbance area, (cm^2).

It can be known from the specific resistance formula that the smaller the tractive resistance and the larger the disturbance area, the smaller the corresponding SDF. This means that the smaller the SDF, the higher the working efficiency of the subsoiler.

Experiment preparation and testing

Test location: School of Mechanical and Electrical Engineering, Inner Mongolia Agricultural University.

The equipment used for providing traction was a trolley. The test takes the Air-Pressure subsoiling shovel as the research object, as shown in Figure 5.

Before the test, the parameters of the soil in the field were measured. Then the soil in the soil trough was treated with a layered treatment method to ensure that the soil parameters in the trough were consistent with those in the field. In this way, the accuracy of the soil trough test could be ensured.

First, 15 cm of soil in the top soil layer was removed and the remaining soil was sprayed with tap water. After the moisture was fully penetrated into the soil, the surface soil was tilled 3 times, and then compacted with rollers. After compaction, the removed soil was backfilled on the soil surface, and the soil was sprayed with tap water in an appropriate amount. After the water has penetrated completely, the soil was repeatedly compacted with roller. In the test, the soil moisture measurement sensor was used to test the humidity of the soil, and the average soil moisture content was maintained at 13%. A firmness sensor was used to measure the soil firmness after each compaction. The soil was compacted repeatedly and the average soil firmness was kept at 2000 N for 0-20 cm soil, and 2500 N for 20-40 cm soil. Soil samples obtained from the trough were taken to the laboratory for determination of soil bulk density.

Fig. 4 - Picture of soil preparation

During the test, the speed of the trolley was 0.5 m/s, and the depth of the subsoiling shovel into the soil was 35 cm. The total length of the soil tank laboratory is 54 m. To leave room for the acceleration and deceleration of the trolley, the soil trough was divided into 3 areas. The actual effective measurement area was 30 m, with 12 m at both ends of the soil trough for acceleration and deceleration.

The test process is shown in Figure 5. In the test, the pressure was provided by the air compressor, connected to the tip of the subsoiling shovel through the air tube, and finally injected into the soil. As shown in Figure 5, the shovel of the Air-Pressure subsoil was fixed on six force suspensions, and connected with the upper pull rod and the trolley by the left and right suspensions. The force sensor on the suspension was connected to the computer on the trolley to transmit tractive resistance data in real time. The air compressor was connected with the shovel by a 6 m air tube.

While the trolley was moving forward and backward, the air compressor was manually pushed to move at the same speed of the trolley, so that the air pressure can be smoothly injected into the soil via the tube. The maximum exhaust pressure was 2.5 MPa, and the rated working pressure was 1.2 MPa.

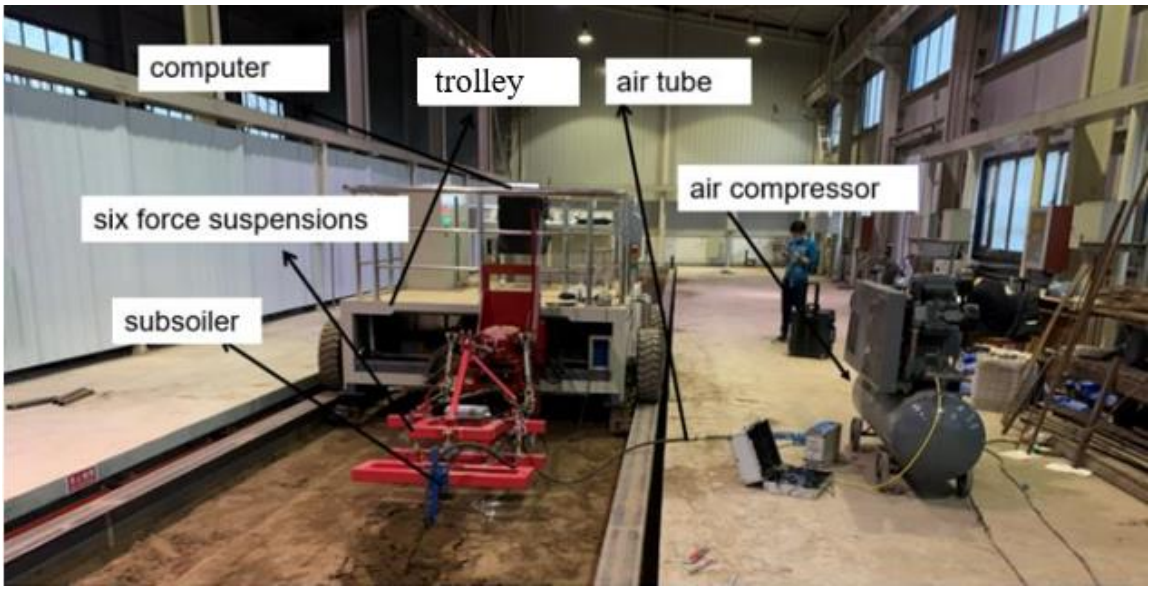

Fig. 5 - Test process

In order to accurately obtain the actual soil disturbance profile of the subsoiling shovel, white ash was marked on the subsoiled ditch according to the soil disturbance test method of Chen et al. (*Hasimu A et al., 2014; Chen Y et al., 2013*) for easy observation. Subsequently, a transparent board was placed on the subsoiled surface and the profile of the soil groove was plotted on the board with a marker. After that, the transparent board was placed on a piece of coordinate paper with an interval of 1 mm, and then the profile was drawn on the paper as shown in Fig. 6(a). The number of squares within the soil groove was the area of the groove. During the test, the tractive resistance of each group of subsoiling shovels was recorded through the six force suspension on the trolley, and the SDF was calculated by the specific resistance formula.

In order to obtain an accurate soil disturbance profile, each measurement was repeated 3 times with an interval of 2 m. To evaluate the subsoiling effect of the Air-Pressure subsoiler more accurately, soil samples before and after subsoiling were taken for soil bulk density determination. Specifically, a pit with a length of 30 cm, a width of 30 cm, and a depth of 50 cm was dug in the soil. Then a cutting ring was used to take three soil samples on the tillage layer, plough pan, and subsoil layer respectively. The cutting ring was then taken out and sealed in a test bag. After subsoiling, the soil samples were taken on both sides of the subsoiling groove with the same method. Each group of tests was repeated 3 times, and the specific sampling process is shown in Figure 6 (b).

(a) (b)

Fig. 6 - Measurement of soil disturbance profile and determination of soil bulk density

RESULTS

The Box-Behnken test was designed based on the above analysis results, and a total of 17 groups of tests were performed, each of which was repeated 3 times. Table 2 shows the design parameters and results of Box-Behnken test. According to the test results, the Design Expert software was applied to establish the second-order regression equation of SDF and variables A (shovel shape), B (pressure magnitude), and C (position of air hole).

The equation is given by:

$$SDF = 4.27 + 0.0065A - 0.4600B + 0.1750C - 0.2550AB - 0.3550AC - 0.0250BC - 0.3035A^2 - 0.2485B^2 + 0.1365C^2 \quad (12)$$

Table 2

Design parameters and results of Box-Behnken test

Serial number	Parameter A (shovel shape)	Parameter B (pressure magnitude)	Parameter C (position of air hole)	SDF (N/cm²)
1	0 (Triangular)	0	0 (The middle part of the shovel)	4.31
2	0	1 (1.2)	-1 (The lower part of the shovel)	3.61
3	-1 (Rectangular)	0	-1	2.91
4	0	0	0	4.01
5	1 (Rhombic)	0 (0.6)	1 (The upper part of the shovel)	4.59
6	0	0	0	4.62
7	-1	1	0	2.79
8	0	-1 (0)	-1	4.36
9	-1	0	1	3.97
10	-1	-1	0	3.32
11	0	0	0	4.31
12	1	0	-1	4.95
13	1	-1	0	5.16
14	1	1	0	3.61
15	0	-1	1	4.76
16	0	0	0	4.11
17	0	1	1	3.91

Analysis of variance was performed on Table 2, and the results are shown in Table 3.

Box-Behnken test analysis of variance **Table 3**

Source of variance	Mean square	Degree of freedom	Sum of squares	P value
Model	0.7748	9	6.97	0.0003
A	3.54	1	3.54	< 0.0001**
B	1.69	1	1.69	0.0002*
C	0.2450	1	0.2450	0.0338*
AB	0.2601	1	0.2601	0.0301*
AC	0.5041	1	0.5041	0.0069*
BC	0.0025	1	0.0025	0.7980
A²	0.3878	1	0.3878	0.0129*
B²	0.2600	1	0.2600	0.0302*
C²	0.0785	1	0.0785	0.1801
Residual	0.0354	7	0.2477	
Lack of Fit	0.0096	3	0.0288	0.9078
Pure Error	0.0547	4	0.2189	
Cor Total	7.22	16		

R2=0.9657; R2adj=0.9216; CV=4.61%; Adeq Precision=15.5959

*Note: ** indicates that the item is extremely significant (p<0.01), and * indicates that the item is significant (p<0.05).*

It can be seen from Table 3 that the shape of the subsoiling shovel (parameter A) has an extremely significant influence on the SDF. The magnitude of air pressure (parameter B) and the position of air hole (parameter C) have a significant impact on the SDF. The effects of interaction terms AB and AC, and the quadratic terms A and B on the SDF are significant. From the perspective of single factor analysis, the influence of each factor on the SDF in descending order is as follows: the shape of the subsoiling shovel (parameter A)> the magnitude of air pressure (parameter B)> the position of air hole (parameter C).

Interaction effect analysis of regression model

The variance analysis results of Box-Behnken test shows that the interaction terms AB and AC have a significant impact on the SDF. Design Expert software was used to draw two interactive response surfaces, as shown in Figure 7.

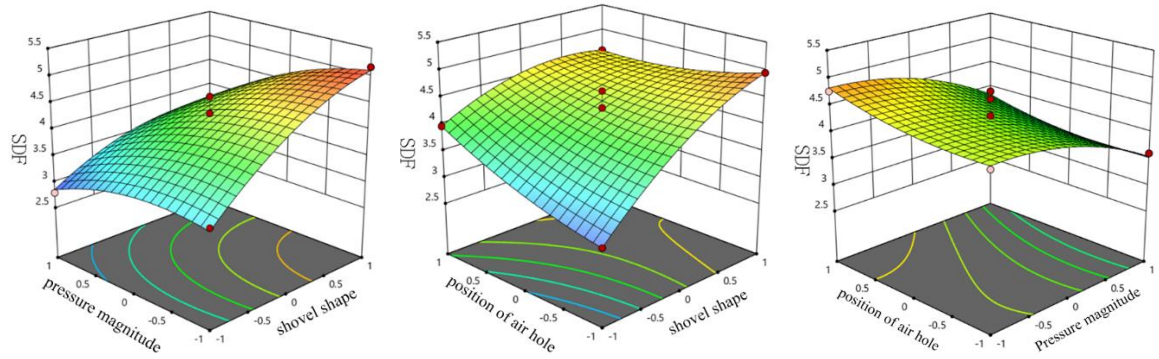

a. A and B interaction *b. A and C interaction* *c. B and C interaction*

Fig. 7 - Interactions between parameters

It can be seen from Figure 7a that the shape of the subsoiling shovel (parameter A)-air pressure magnitude (parameter B) corresponds to a large slope of the curved surface, which causes a large change in the SDF. And the contour line shows a large curvature. These indicate a strong interaction between parameter A and parameter B. Figure 7b shows that the surface slope corresponding to the shape of subsoiling shovel (parameter A)-air hole position (parameter C) is relatively large, indicating that parameters A and C have a great impact on SDF. The contour line in Figure 7b shows a large curvature, indicating that the interaction between the shovel shape (parameter A) and the magnitude of air pressure (parameter B) is significant. It can be seen from Figure 7c that the position of air hole (parameter C) and the magnitude of air pressure (parameter B) are flat, indicating that the interaction effect is insignificant.

Optimal parameters and comparative analysis

The optimization function of Design Expert was used to obtain the minimum SDF, and several groups of solutions were obtained. The optimal solution is as follows: The shape of the subsoiling shovel is rectangular, the air pressure is 1.2 MPa, and the air hole is located on the upper part of the subsoiling shovel.

The new Air-Pressure subsoiler was compared with the traditional Air-Pressure subsoiler by the soil tank test method under the same test factors. The tractive resistance and soil disturbance after subsoiling were recorded, as shown in Figure 8.

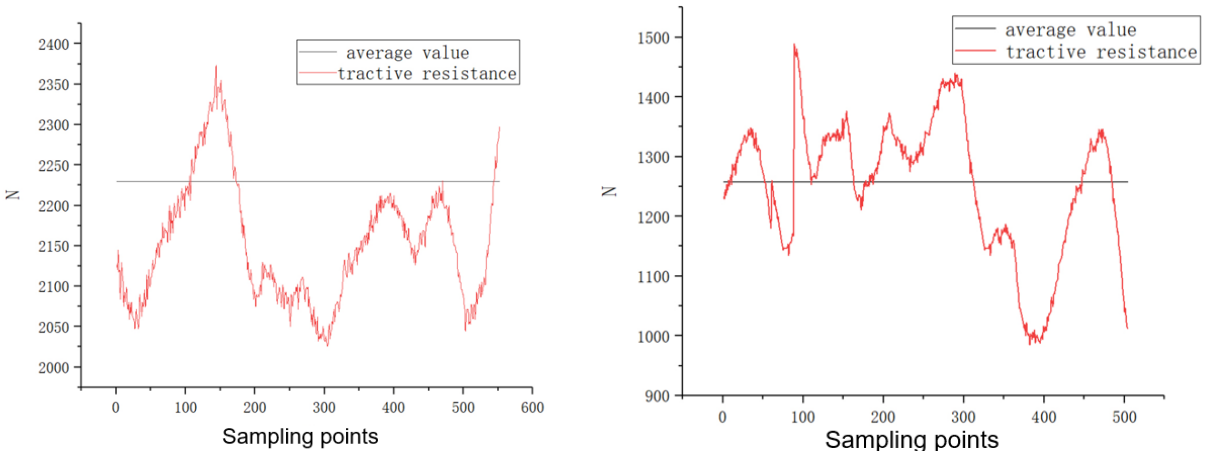

The traditional Air-Pressure subsoiler *The new Air-Pressure subsoiler*

Fig. 8 - Tractive resistance

It can be clearly seen from Figure 8 that the traction resistance of the new subsoiler is reduced by 44.08% compared to the traditional one. It can be calculated that the SDF of subsoiling is reduced by 12.7%.

The soil bulk density before and after subsoiling by the new Air-Pressure subsoiler is shown in the table below. It can be seen from the table that the average bulk density of soil before subsoiling is 11.1% lower than that after subsoiling.

Change of soil bulk density **Table 4**

Soil bulk density (g/cm^3)	The first time	The second time	The third time	Mean
Before subsoiling	1.32	1.36	1.38	1.35
After subsoiling	1.19	1.22	1.21	1.20

CONCLUSIONS

This paper establishes the force model of the shovel surface of the Air-Pressure subsoiler and the soil under the action of air pressure, and analyses the mechanism of the Air-Pressure subsoiler in soil splitting and resistance reduction. Moreover, this paper deduces the formula for calculating the tractive resistance of this proposed subsoiler during operation. It is found that increasing the air pressure can effectively reduce the tractive resistance.

Through a comprehensive analysis of factors such as soil characteristics, groove area, and subsoiling resistance F, it is found that the shape of the subsoiling shovel has the most significant influence on the SDF. Among the three types of shovel, the Air-Pressure subsoiler with a rectangular subsoiling shovel has the largest disturbance to the soil and the smallest tractive resistance. The bulk density decreases by 11.1% on average.

Under the test conditions of this study, the Air-Pressure subsoiler with a rectangular shovel and an entry angle α of 21° is the best subsoiler.

When the pressure is 1.2 MPa and the air hole is in the upper part of the shovel, the subsoiling performance is the best. Compared with the original Air-Pressure subsoiler, the newly-designed Air-Pressure subsoiler reduces the tractive resistance by 44.08%, and the SDF by 12.7%.

ACKNOWLEDGMENT

The supports of the National Natural Science Foundation of China (NSFC) (No. 51905277), and the financial support the Inner Mongolia Natural Science Foundation (No. 2019BS05014), High-level Talent Scientific Research Project of Inner Mongolia Agricultural University (No. NDYB2018-7) for this research are greatly appreciated.

REFERENCES

[1] An Jing, (2016). *Soil compaction mechanisms of black soil and brown earth in the Northeast of China* (*东北地区棕壤和黑土旱田土壤板结机理研究*) Ph.D. Thesis, Shenyang Agricultural University.

[2] Bandalan, E. P., Salokhe, V. M., & Gupta, C.P. (1999). Performance of an oscillating subsoiler in breaking a hardpan. *Journal of Terramechanics*, 36(2), 117-125.

[3] Chen Y., Munkholm L.J., & Nyord T. (2013). A discrete element model for soil–sweep interaction in three different soils. *Soil & Tillage Research*, 126(none), 34-41.

[4] Guo Jinlong. (2016). *Design and research of vibration subsoiler* (master's degree thesis, Shihezi University)

[5] Gao Xiaodong. & Pei Xinmin. (2015). Current situation and problems of subsoilers at home and abroad. (玉米免耕播种深松联合作业机研究). *Agricultural Machinery* (21), 89-91.

[6] He Jin. (2005). *Study on Drilling and Subsoiling Combined Machine for No-till Maize (玉米免耕播种深松联合作业机研究)* (Master's Degree Thesis, China Agricultural University).

[7] Hilal Y.Y., Al-rajabo Saad Abdul Jabbar & Dahham G. A. (2021). The effects of vibrating wings subsoiler plough on driver's seat of agricultural tractors and mechanization performance. *Soil and Tillage Research*, 205, 104806.

[8] Hasimu A., & Chen Y. (2014). Soil disturbance and draft force of selected seed openers. *Soil & Tillage Research*, 140, 48-54.

[9] Liu Mingcai. (2018). *The design and research of the dry land pressure deep pine machine (旱作耕地气压深松机的设计与研究)* (master's thesis, Fujian Agriculture and Forestry University).

[10] Liu Jun'an, Wang Xiaoyan, Li Hongwen, He Jin, Wang Qingjie & Li Wenying. (2017). Structural parameter optimization of subsoiler based on soil disturbance and traction resistance (基于土壤扰动与牵引阻力的深松铲结构参数优化). *Journal of Agricultural Machinery* (02), 60-67.

[11] Mechanical Research Institute of the First Ministry of Machinery. (1973). *Agricultural Machinery Design Manual（农业机械设计手册）*. Mechanical Industry Press.

[12] Schuring J.R., Jurka V., & Chan P.C. (2010). Pneumatic fracturing to remove VOCS *Remediation Journal, 2*(1), 51-68.

[13] Niyamapa T. and Salokhe V.M. (2000). Force and pressure distribution under vibratory tillage tool. *Journal of Terramechanics*, 37(3), pp. 139-150.

[14] Wang Y., Osman A.N., Zhang D., Yang L., & Zhong X. (2019). Optimized design and field experiment of a staggered vibrating subsoiler for conservation tillage. International *Journal of Agricultural and Biological Engineering*, 12(1), 59-65.

[15] Zuo Shengjia, Kong Degang, Chinese, Chen Haixia, Zhang Yong & Han Fuao, (2017). Research status and development trend of pneumatic subsoiling technology (气压深松技术研究现状和发展趋势). *Chinese Journal of Agricultural Machinery Chemistry* (06), 99-103.

[16] Zhang Siyuan. (2018). *Design and Experimental study on the Forced Vibration Subsoiler (受迫振动深松机的设计与研究)* (master's degree thesis, Shihezi University).

[17] Zuo Shengjia, Kong Degang, Chen Haixia, Chinese, Zhang Yong & Liu Chunsheng. (2017). Pneumatic subsoiler design based on pneumatic fracturing theory (基于气压劈裂原理的气压深松机设计). *Journal of Chinese Agricultural Mechanization* (04), 5-10.